

EARLY TYPE GALAXY CORE PHASE DENSITIES

R. G. CARLBERG

Department of Astronomy and Astrophysics, University of Toronto, Toronto, ON M5S 3H4, Canada

F. D. A. HARTWICK

Department of Physics and Astronomy, University of Victoria, Victoria, BC V8W 3P6, Canada

Draft version April 17, 2014

ABSTRACT

Early type galaxies have projected central density brightness profile logarithmic slopes, γ' , ranging from about 0 to 1. We show that γ' is strongly correlated, $r = 0.83$, with the coarse grain phase density of the galaxy core, $Q_0 \equiv \rho/\sigma^3$. The γ' -luminosity correlation is much weaker, $r = -0.51$. Q_0 also serves to separate the distribution of power-law profiles, $\gamma' > 0.5$ from nearly flat profiles, $\gamma' < 0.3$, although there are many galaxies of intermediate slope, at intermediate Q_0 , in a volume limited sample. The transition phase density separating the two profile types is approximately $0.003 \text{ M}_\odot \text{ pc}^{-3} \text{ km}^{-3} \text{ s}^3$, which is also where the relation between Q_0 and core mass shows a change in slope, the rotation rate of the central part of the galaxy increases, and the ratio of the black hole to core mass increases. These relations are considered relative to the globular cluster inspiral core buildup and binary black hole core scouring mechanisms for core creation and evolution. Globular cluster inspiral models have quantitative predictions that the data support, but no single model yet completely explains the correlations.

1. INTRODUCTION

Early type galaxies, ellipticals and S0s, form an impressively regular sequence with luminosity, as seen in the Faber-Jackson relation (Faber & Jackson 1976) and generalized in the fundamental plane relations (Djorgovski & Davis 1987; Binney & Merrifield 1998). The core radius and brightness are basic observational properties which hold clues to the origin of the early type galaxies. Galaxy merging, star-formation, the presence of black holes and, in sufficiently dense cores, dynamical friction and two-body relaxation, all play some role in creating the cores. One widely considered possibility for the formation and evolution of early type galaxy cores is that they are largely a result of stellar dynamical processes in the core with gas and star formation playing minor roles.

The coarse grain phase space density can be defined as $Q_0 \equiv \rho_0 \sigma_0^{-3}$. Q_0 is a key dynamical quantity to assess the relative roles of various stellar dynamical processes. The local phase density controls the rate of two-body relaxation and dynamical friction, along with the masses of the orbiting bodies (Binney & Tremaine 2008). Liouville's theorem (Goldstein et al. 2002) requires that the fine grain phase density, F , is a constant of the motion in a conservative Hamiltonian system, with the coarse grain phase density required to be $Q \leq F$ (with appropriate velocity space normalization).

The observational description of the central surface brightness distribution of early type galaxies began with ground-based telescope data and used the physically well motivated King model (King 1962, 1966, 1978). CCDs observations showed that some early type galaxies, particularly those with lower luminosities, had central brightness distributions that rose above the con-

stant brightness King model core (Kormendy 1985; Lauer 1985) although earlier photographic data had noted this as indicating the presence of a stellar nucleus (Binggeli et al. 1984). The angular resolution of the Hubble Space Telescope showed that what became known as power-law cores were increasingly common with decreasing galaxy luminosity. (Crane et al. 1993; Ferrarese et al. 1994; Kormendy et al. 1994).

The central density profiles of early type galaxies are classified as being a power-law, if the negative logarithmic slope is greater than 0.5, or, cored, if the slope is shallower than 0.3 (Gebhardt et al. 1996; Ravindranath et al. 2001; Rest et al. 2001; Lauer et al. 2007b). However, the core parameters and the degree of bimodality of the central slope distribution depend on the surface brightness fitting model and the sample definition.

The purpose of this paper is to calculate the phase density of spheroidal systems, focusing on early type galaxies, to consider its correlations with core properties. In particular we examine to what degree phase density relates to the suggestions that early type cores have a bimodal distribution in their brightness profile slopes. These relations are considered as tests of stellar dynamical models for the formation and evolution of early type galaxy cores.

2. THE OBSERVATIONAL DATA

There are two leading functional forms to fit a general core brightness profile. The Nuker formula (Lauer et al. 1995; Carollo et al. 1997; Lauer et al. 2007b) is designed to describe the central region of a galaxy and does not need data at large radii, which is often convenient if there is limited observational coverage. An alternate, whole galaxy, brightness profile fitting approach is the core-Sérsic function (Graham & Guzmán 2003; Graham et al. 2003; Trujillo et al. 2004; Ferrarese et al. 2006; Turner et al. 2012; Dullo & Graham 2012). The core-Sérsic func-

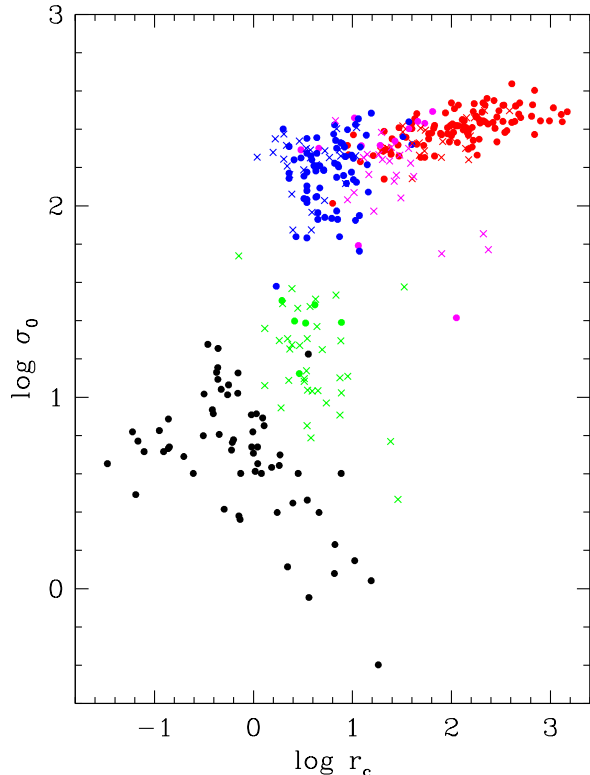


FIG. 1.— The core velocity dispersions and r_c values fitted for early type galaxies from the Lauer et al. (2007b) (points) and ATLAS3D (crosses) samples. with cores (red), intermediate slopes (magenta) and power-law cores (blue), late type galaxy nuclear star clusters (green points and crosses) and globular clusters (black points).

tion provides good fits to the entire brightness profile of a galaxy at the relatively small cost of a single extra parameter. There are significant differences of detail between the two approaches and no clear consensus on best approach has emerged.

The slope of the brightness profile at the smallest practical radius of observation, $0.1''$, defines the parameter γ' of the Nuker approach. The angular definition introduces a direct distance dependence in the measurement. The Nuker γ' is in general agreement with the core-Sérsic measurement of the comparable quantity, although with some scatter and a systematic offset (Dullo & Graham 2012). The fitted break radius of the Nuker profile has limitations in describing the core radius (Carollo et al. 1997) which led to the development of a transformed quantity, r_γ , the radius at which the Nuker fit has a slope of 0.5, as the best measure of the core radius. Dullo & Graham (2012) show that the core-Sérsic break radius, $r_{b,cS}$, is in good agreement with the Nuker r_γ .

Defining a representative sample of early type galaxies is important when comparing trends within a population. The Lauer et al. (2007b) sample is the largest available compilation and is approximately magnitude limited. A very wide ranging set of kinematic and dynamical data are available for the ATLAS3D Cappellari et al. (2011) sample, which is designed to be a complete

volume limited sample. Both samples report Nuker profile fit parameters and serve as two large, comparable and complementary samples for our analysis.

2.1. Phase Density Calculation

To calculate the core coarse grain phase space density requires measurements of the core velocity dispersion and core radius, from which other quantities can be derived. The different types of systems have a range of density profiles and somewhat different approaches to measurement are used, meaning that the phase densities will have small systematic differences between them although we expect these to be much smaller than the large range of Q_0 values present. To obtain a physical mass density in the core we use the King radius relation (Binney & Tremaine 2008) of a non-singular isothermal sphere for all systems,

$$\rho_0 = \frac{9}{4\pi G} \frac{\sigma_0^2}{r_c^2}. \quad (1)$$

We recognize that few of the systems are particularly well described as an isotropic isothermal sphere, however Equation 1 provides a uniform basis to calculate basis that will be correct within a factor of a few. To employ Equation 1 we need to identify a central velocity dispersion and a measure of the core radius for the systems that we consider. Although our primary interest is the early type galaxies, in which core radii are measured in the same way, we will make comparisons to phase densities of nuclear star clusters of late type galaxies and globular clusters in which the measures of core radius are comparable but not identical, which will lead to systematic differences, but these will not affect our limited use.

Given our assumptions,

$$Q_0 = \frac{166.6}{\sigma_0 r_c^2} \quad (2)$$

for σ_0 in units of km s^{-1} and r_c in units of pc. Q_0 is the approximate phase space density at the core radius and normally increases inward from that location.

2.2. Early type Galaxies

The Lauer et al. (2007a,b) sample is a large compilation of available HST data, but as an approximately apparent magnitude limited sample contains more luminous galaxies than a volume limited sample (Lauer et al. 2007b; Côté et al. 2007). In total there are 189 galaxies in the sample that have core profiles and central velocity dispersions.

The ATLAS3D sample (Krajnović et al. 2013) is constructed to be essentially a complete sample of galaxies more massive than about $6 \times 10^9 M_\odot$ within 42 Mpc. Krajnović et al. (2013) provides Nuker fits for the surface brightness profiles. We remove galaxies with upper limits for r_γ from the sample, which reduces the numbers to 74. We equate r_γ with r_c below. For the ATLAS3D sample we use the values of velocity dispersion at $R_e/8$ as tabulated in Cappellari et al. (2013).

For all early type galaxies we calculate the core mass from the projected quantities, using the relationship $\Sigma_0 = 2\rho_0 r_c$,

$$M_c = 4\pi\rho_0 r_c \int_0^{r_c} r(r/r_c)^{-\gamma'} dr. \quad (3)$$

This integrates to $M_c = 4\pi\rho_0 r_c^3/(2 - \gamma')$.

Density profiles are classified as being cored if $\gamma' < 0.3$ (red in plots) and power-law if $\gamma' > 0.5$ (blue in plots), with an intermediate type between (magenta in plots) (Lauer et al. 2007b).

2.3. Globular clusters

Globular clusters may play a significant role in the formation of galactic cores (Tremaine et al. 1975). Accordingly it is interesting to understand where their phase densities fits into the overall sequence (Walcher et al. 2005). In this work we will assume that the Milky Way globular clusters are representative of the group as a whole. For these clusters, core radii and central velocity dispersions come from the 2010 edition of the compilation of Harris (1996). In the following figures globular cluster data are plotted as solid black dots.

We use Equation 1 to calculate the core density. We approximate the core to be constant density, so the core mass is,

$$M_c = \frac{4\pi}{3} \rho_0 r_c^3. \quad (4)$$

2.4. Disk Galaxy Nuclear Star Clusters

The data for the nuclear star clusters in disk galaxies comes from the work of Böker et al. (2004) and Walcher et al. (2005), who also estimated phase space densities at the half-mass radius. There are six galaxies in Table 3 of Walcher et al. (2005) for which values of the profile fitted r_e are available in the Böker et al. (2004) paper. Densities for these galaxies were calculated using Equation 1 above but with $r_c \equiv r_e/0.75$ (that is, the r_h of Walcher et al. (2005)). This identification of core radius effectively considers the entire NSC to be a core. Depending on the concentration of the core, the phase density can be several times higher. Under this assumption, Q_0 for each galaxy can then be calculated from the tabulated values of σ . In the figures these six galaxies are plotted as solid green dots. For the remaining galaxies in the Böker et al. (2004) Table 1 with r_e values, core masses were calculated from the given luminosities and an assumed M/L of 0.5 which is the median value in Table 3 of the Walcher et al. (2005) paper. Velocity dispersions were obtained using the following empirically determined relation by fitting to the data in Table 3 of Walcher et al. (2005),

$$\sigma_0^2 = 0.45 \frac{GM_c}{r_e}. \quad (5)$$

The resulting empirically determined values of Q_0 are plotted as green crosses in the figures.

The data are plotted in the r_c vs σ_0 observational plane in Figure 1. Power-law cores are plotted as blue dots and cored galaxies as red dots. We note that in this plot the various types of objects have substantial overlap when projected onto any one axis. There is also substantial mass overlap between the various object types.

3. Q_0 DEPENDENCE OF CORE SLOPE

In Figure 2 we plot the core phase densities as a function of their inner brightness profile slope, γ' , for all early type galaxies for both the Lauer et al. (2007b) and Krajnović et al. (2013) samples. A strong correlation between the log of Q_0 and γ' is readily visible. The Pearson

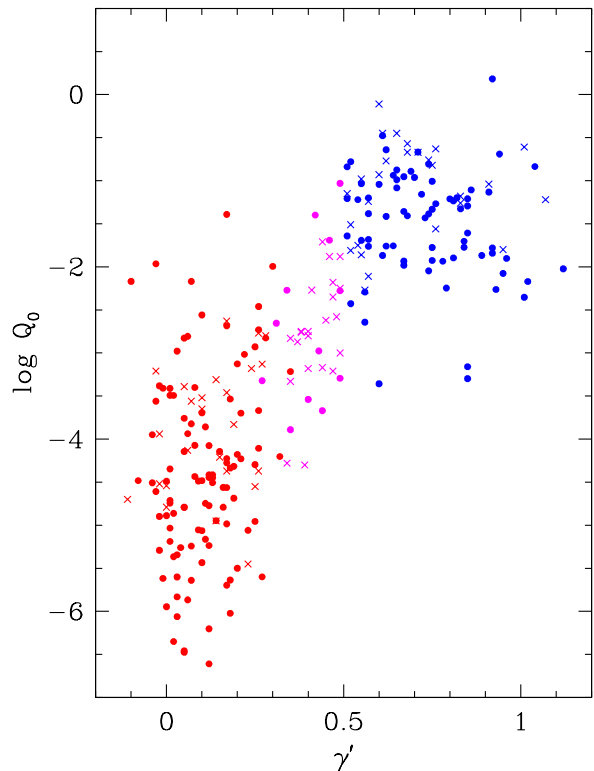


FIG. 2.— The central phase density, ρ_0/σ_0^3 , in units of $M_\odot \text{pc}^{-3} \text{km}^{-3} \text{s}^3$ of early type galaxies as a function of the logarithmic slope of the surface brightness near the center. The points have the same colors as in Fig. 1. The Lauer et al. (2007b) sample is shown with colored dots and the ATLAS3D sample is shown with crosses.

linear correlation coefficients for the $Q_0 - \gamma'$ correlation is 0.78 for the Lauer et al. (2007b) sample and 0.83 for the Krajnović et al. (2013) sample. That is, the core phase space density explains an impressive 69% ($= r^2$) of the variance in γ' . The correlation of γ' with luminosity is fairly weak in the ATLAS3D sample, -0.51 , *i. e.* only about 25% of the variance, where we use the log of the r band luminosities, L_r , of Cappellari et al. (2013). The correlation of $\log Q_0$ and either log of the stellar mass or r band luminosity is also comparably weak, $r = -0.49$ and -0.50 , respectively. The weak correlation with the total mass or luminosity of the galaxy indicates that although early type cores evolve within their host galaxy, the host galaxy does not completely control the resulting core properties.

To further explore the correlation of core density profile and the bimodality proposals, Figures 3 and 4 show for the two early type samples the distribution of their core and power-law types, $\gamma' < 0.3$ and $\gamma' > 0.5$ respectively, as a function of their phase space density. Remarkably Q_0 fairly cleanly separates the cored and power-law ellipticals into two almost non-overlapping distributions. The relative numbers of core and power-law galaxies are comparable in both samples. Of the 25 cored and 26 power-law galaxies in the Krajnović et al. (2013) sample, only one from each falls into an overlapping region of Q_0

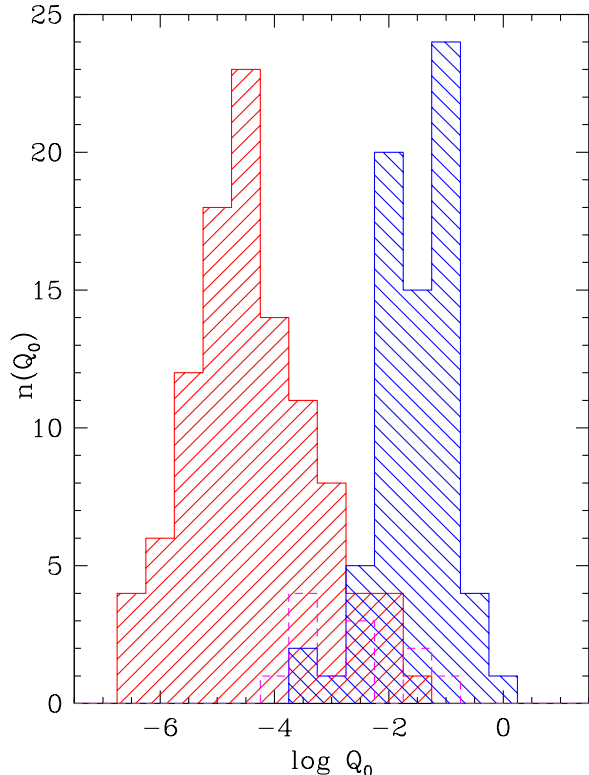


FIG. 3.— The phase space density distribution of early type galaxies classified as cored (red), intermediate (magenta) and power-law (blue) from the Lauer et al. (2007b) sample.

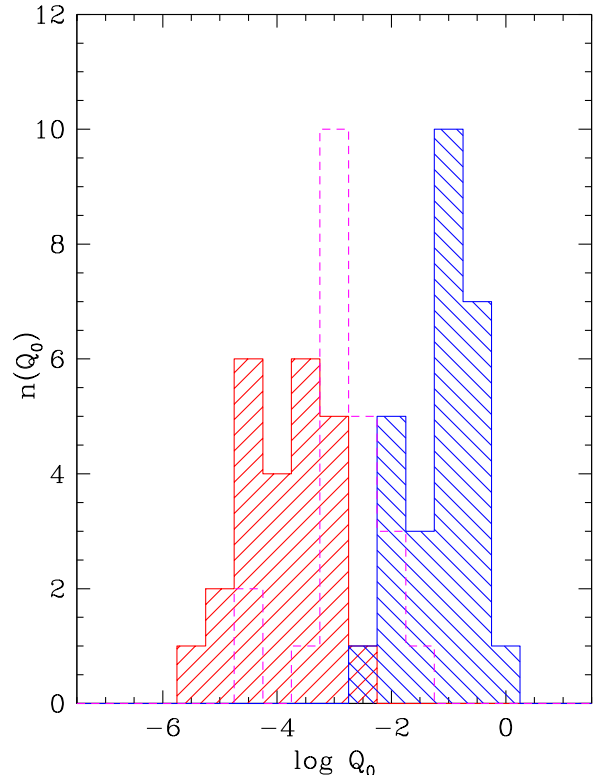


FIG. 4.— Same as Figure 3 but for the volume limited Krajnović et al. (2013) sample.

in Figure 4.

The intermediate core types, those with $0.3 \leq \gamma' \leq 0.5$, fill in the Q_0 region between the cored and power-law types. The intermediate core slope population is relatively large in the Krajnović et al. (2013) sample, 22 of the 74, with 11 of the 189 in the Lauer et al. (2007b) sample, likely reflecting the difference between the sample selection criteria. Although it is true that cored and power-law galaxies do form two nearly non-overlapping distributions in Q_0 , a more physical interpretation is that γ' is a continuous variable that is strongly ordered with the core Q_0 . We note that the transition from power-law to cored galaxies occurs near $Q \simeq 0.003 M_\odot \text{pc}^{-3} \text{km}^{-3} \text{s}^3$.

4. DYNAMICAL QUANTITIES AND Q_0

4.1. Core Mass

The core phase densities of early type galaxies, nuclear star clusters and globular clusters are shown in Figure 5 as a function of the calculated core mass. As a group the objects appear to form a single sequence in this particular dynamical space. There is a distinct break in the slope between cored and power-law galaxies.

We know about what to expect for a $Q_0 - M_c$ relation. Equations 2 and 4 give $Q_0 \propto \sigma_0^3 M_c^{-2}$. If we take a Faber-Jackson relation for the core to be, $\sigma_0 \propto M_c^\beta$ and use Equation 1 to eliminate the density, then

$$Q_0 \propto M_c^{-2+3\beta}. \quad (6)$$

The power-law cores in Figure 5 have a $Q_0 - M_c$ slope from 72 points -1.109 ± 0.064 whereas the 105 cored early type galaxies have -1.641 ± 0.025 . Kormendy & Bender (2013) find Faber-Jackson relationships, $L_v \propto \sigma_0^n$, where their $n = 1/\beta$, or $n \simeq 3.74$ for power law galaxies and 8.33 for cores, assuming that the core mass is directly proportional to the total luminosity, which is approximately true as shown in Figure 6. Accordingly we would expect $Q_0 - M_c$ slopes of -1.20 and -1.64, consistent with the fitted relations, for power-law and cored early types, respectively. The correlation between Q_0 and M_c has $r = 0.95$. However Q_0 is better predictor of γ' , with 81% confidence that the increased correlation of $\gamma' - \log Q_0$ over $\gamma' - \log M_c$ is significant.

4.2. Rotation

Lauer (2012) showed that core type correlates well with the rotation parameter calculated from the sub-sample of ellipticals with rotation maps (Emsellem et al. 2004). The kinematic data has been obtained with ground based telescopes so does not have the angular resolution of the imaging data. However, it remains of considerable interest to compare the core phase space density with rotation properties at a larger radius. Figure 7 shows the correlation of the rotation parameter values of Emsellem et al. (2011) measured within $R_e/2$ and the ATLAS3D Q_0 values. There is a range of rotation at every Q_0 , with a growing maximum rotation with increasing Q_0 . The $Q_0 - \lambda_{Re/2}$ correlation coefficient is 0.55. Factors other

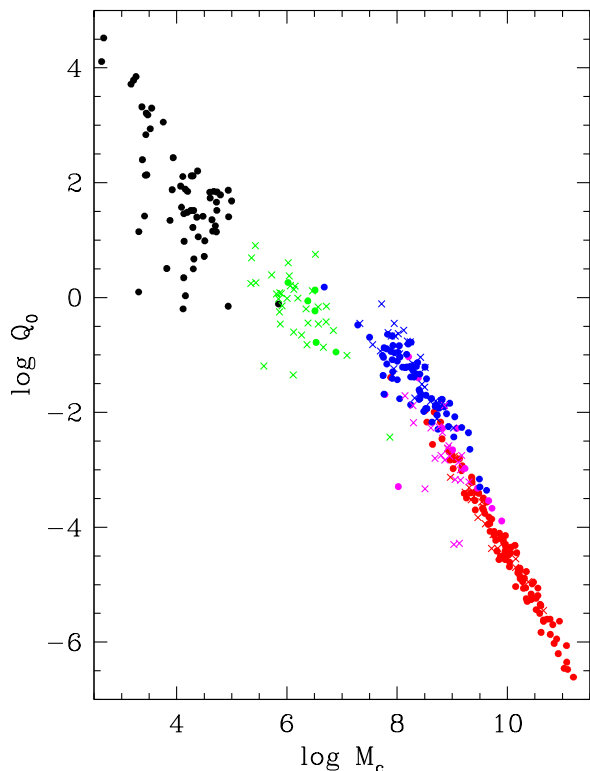


FIG. 5.— The central phase density, ρ_0/σ_0^3 , in units of $M_\odot \text{pc}^{-3} \text{km}^{-3} \text{s}^3$. The points have the same colors as in Fig. 1.

than Q_0 dominate the rotation value for an individual galaxy, which is hardly surprising given that a significant range in the initial angular momentum is expected. However Q_0 usefully indicates the mean rotation, with a value of 0.38 ± 0.03 above the critical value of $Q_0 = 0.003$ whereas it is 0.21 ± 0.03 below.

We note that the ATLAS3D sample we are using contains a number of kinematically distinct cores (KDC) defined on the basis that the kinematic axis changes by at least 30° (Krajnović et al. 2011). For our sub-sample one KDC occurs in an intermediate core type, the 8 others are in cored galaxies, consistent within the small numbers with the expected fraction of about half the cored galaxies.

4.3. Dark Matter Fraction

It is straightforward to undertake a principal component analysis (PCA) using the R project software (<http://www.r-project.org/>). We remove strongly correlated variables, leaving the PCA with γ' , the r band luminosity, and the parameters reported in Cappellari et al. (2013), the flattening at $Re/2$, the rotation parameter within $Re/2$, the kinematic/photometric misalignment angle, ψ , and f_{DM} , the dark matter fraction inside Re . The PCA finds that the first component provides 49% of the variance, and three components of seven are required to provide 80% of the variance. The PCA confirms that Q_0 is the single most strongly correlated variable with γ' . However the next most correlated variable

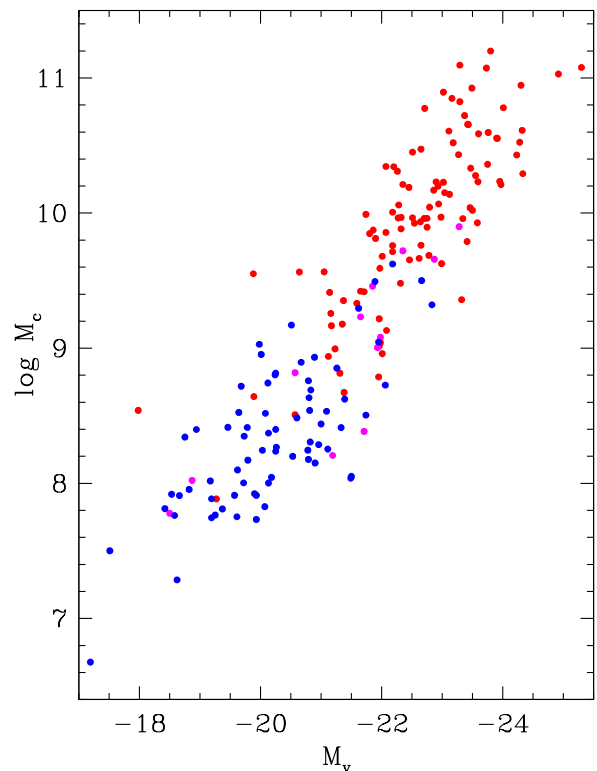


FIG. 6.— The core mass as a function of luminosity for the Lauer et al. (2007b) sample. Symbols are as in Figure 1.

is the dark matter fraction, f_{DM} , as evaluated at Re . A general linear model fit finds $\gamma' = (0.138 \pm 0.015) \log Q_0 - (0.32 \pm 0.12) f_{DM} + (0.25 \pm 0.10) \lambda_{Re/2} + 0.745$. The f_{DM} term has a probability of only 0.8% of chance occurrence and the rotation term $\lambda_{Re/2}$ has a probability of 1.6% of chance occurrence. However, $\log Q_0$ removes about 69% of the variance, whereas both f_{DM} and rotation each account for only about 2.3%, leaving 26% unaccounted. The negative correlation with γ' indicates that a lower dark matter fraction is associated with power-law cores. This is suggestive that somewhat more dissipated galaxies, hence lower dark matter fraction, are more likely to have steep core profiles at the same Q_0 , but it is a small effect.

4.4. Central Super-Massive Black Holes

Super-massive black holes are closely connected to galaxy cores although the evolutionary dependence is not entirely clear. There are well known correlations between the velocity dispersion of ellipticals and their black holes (Magorrian et al. 1998; Ferrarese & Merritt 2000; Gebhardt et al. 2000). Black hole masses are available in Graham & Scott (2013) and McConnell & Ma (2013). Although the galaxies with black-hole masses are a subset of those with core density measurements, there is no clear bias other than the size and distance considerations needed to allow a black hole mass measurement. Figure 8 shows the ratio of the derived black hole mass to our estimated core masses as a function of their core phase den-

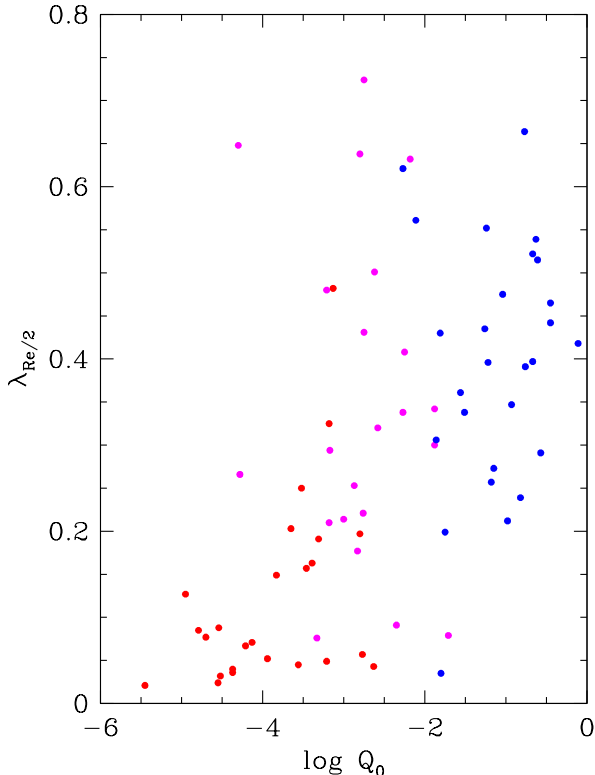


FIG. 7.— The rotation parameter as a function of the phase space density for the ATLAS3D sample.

sities. The high Q_0 , power-law core, galaxies have core masses comparable to the black hole mass, with a median $M_{BH}/M_c \simeq 0.5$. That is, the cores of most galaxies with $Q_0 > 0.003 \text{ M}_\odot \text{ pc}^{-3} \text{ km}^{-3} \text{ s}^3$ are within the black holes sphere of gravitational influence (Milosavljević & Merritt 2001). Cored galaxies have much more massive cores on the average, with a median value $M_{BH}/M_c \simeq 0.1$.

5. IMPLICATIONS OF CORE PHASE DENSITIES

5.1. Dynamical Times in Dense Cores

The phase space density determines the time for two-body relaxation (Binney & Tremaine 2008). We adopt the parameter choices of Merritt (2013), his Equation 5.61, to find,

$$t_2 = \frac{1.1 \times 10^9 \text{ M}_\odot}{Q} \frac{15}{m \ln \Lambda} \text{ yr.} \quad (7)$$

A relaxation time of 10^9 yr for a population of $m = 1 \text{ M}_\odot$ stars occurs for $Q = 1.1$. The power-law cores containing black holes shown in Figure 8, have median $Q_0 \simeq 0.1$, in which case interaction with two-body relaxation of stars around the black-hole likely plays a significant role in building and maintaining a power-law core (Merritt & Szell 2006).

The time scale for dynamical friction depends linearly on the phase space density and the mass of the inspiraling satellite (Binney & Tremaine 2008). We again use the parameters of Merritt (2013), his Equation 5.32,

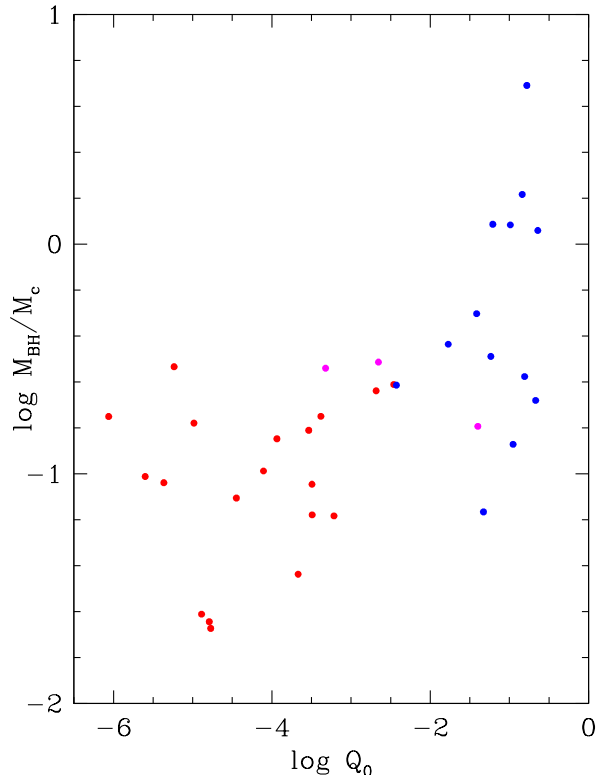


FIG. 8.— The ratio of the central black hole mass to the core mass as a function of Q .

to give the radial dependence of the dynamical friction timescale,

$$t_{df}(r) = \frac{1.4 \times 10^{10}}{Q(r)} \frac{0.35 \text{ M}_\odot}{G(x)} \frac{10}{m \ln \Lambda} \text{ yr} \quad (8)$$

where $G(v/\sigma)$ is a slowly varying function with a value of 0.347 for $v/\sigma = \sqrt{2}$, roughly as expected for an inspiralling satellite. For a somewhat heavy $3 \times 10^5 \text{ M}_\odot$ globular cluster to spiral in within a 10^{10} years requires that it orbit in a region with a local $Q > 4 \times 10^{-6} \text{ M}_\odot \text{ pc}^{-3} \text{ km}^{-3} \text{ s}^3$. Therefore, the most massive early type galaxies, those with cores more massive than about 10^{10} M_\odot (Figure 5) only allow globulars more massive than $3 \times 10^5 \text{ M}_\odot$ to spiral into the center.

5.2. Core Phase Density Evolution Pathways

A successful core formation and evolution scenario needs to offer a way to understand the correlations presented here between the core phase density and its brightness profile, rotation and black hole mass. High redshift progenitor galaxies may largely form with power-law cores through dissipative star formation processes (Loose et al. 1982) although current specific models appear to create too steep a Faber-Jackson relation (McLaughlin et al. 2006; Antonini 2013). A widely investigated approximation, which we will follow, is to assume that the stars in the cores of early type galaxies were largely created elsewhere and brought to the core through merging

and dynamical friction and possibly had their density profile altered through two-body relaxation. Here we briefly examine to what degree these stellar dynamical processes can account for the phase space correlations of core properties. Two widely discussed and quite distinct ideas are either that early type galaxies began with large low density cores which were subsequently built up, or, they were formed with power law cores, which were subsequently scoured out in the more massive galaxies. Both mechanisms may be at work.

The slope of the power-law cores in the $Q_0 - M_c$ diagram, Figure 5, appears to be a continuation of the trendline from globular clusters through Nuclear Star Clusters. Precisely the same data are multiplied with its core mass squared to remove the basic mass dependence of Equation 6. The rescaled results are displayed in Figure 9 which helps make the idea of two sequences clearer. Shown on the plot is a line of constant density, under the self gravitating virial assumption, which gives $\sigma^2 \propto M_c^{2/3} \rho^{1/3}$ and therefore $Q_0 M_c^2 \propto \rho^{1/2} M_c$.

N-body simulations for the bulk of the galaxy find $\beta \simeq 0.3$ for equal mass mergers and $\beta \simeq -0.3$ for minor mergers (Naab et al. 2009; Hilz et al. 2012), although these values will not necessarily strictly apply to the cores. Recall that we have translated the Faber-Jackson relation to $Q_0 M_c^2 \propto M_c^{3\beta}$. The shallow trend of the cored early types in Figure 9 is highly suggestive that *major* merging dominates the evolution of these cores, with some admixture of minor merging to flatten out the relation, as has been noted from their Faber-Jackson relations (Kormendy & Bender 2013). If the merging were predominantly minor mergers it would cause $Q_0 M_c^2$ to decline with increasing core mass, which is not seen. It is also suggestive that a steeper trend continues through power-law cores as has been previously noted (Walcher et al. 2005; Côté et al. 2007; Glass et al. 2011). The globular cluster core densities are set through star formation processes and subsequent dynamical evolution. The globular cluster inspiral process will dissolve the clusters when the mean interior density of galaxy core and the cluster are equal, that is, the mass buildup will tend to push the increasing mass objects along a roughly constant density line, (Capuzzo-Dolcetta & Miocchi 2008; Hartmann et al. 2011). A sequence of infall events leads to a modest increase in central density (Antonini et al. 2012). The presence of a central black hole complicates the process but the general trends remain (Antonini 2013).

5.2.1. The Power-law Core Buildup Scenario

Although not necessarily the only mechanism which creates shallow cores, one interesting possibility is that most of the stars in early type galaxies may have been formed in galactic disks, either isolated or in star bursts associated with merging. Subsequent merging of the stellar components leads to a core phase density that is no higher than the phase density of the central regions of the merging disks (Toomre & Toomre 1972; Barnes 1988; Cox et al. 2006).

Genzel et al. (2011, 2014) presents observational measurements of star forming galaxies near redshift two. The phase space density of a disk is $Q_d = \Sigma / (2h\sigma^3)$, using our normalization and where Σ is the local surface density, h the scale height, and σ the velocity dispersion which

we will take to be isotropic for simplicity. Taking high redshift disk parameters of $\Sigma \simeq 2-3 \times 10^3 \text{ M}_\odot \text{ pc}^{-2}$ (with some fraction as stars), $z_0 \simeq 300 \text{ pc}$, and $\sigma \simeq 80 \text{ km s}^{-1}$ (Genzel et al. 2011), which gives a representative central disk $Q_0 \simeq 3 \times 10^{-6} \text{ M}_\odot \text{ pc}^{-3} \text{ km}^{-3} \text{ s}^3$. The Milky Way has a comparable central phase density. Merging such stellar disks would create an initial core $Q_0 \simeq 10^{-6} \text{ M}_\odot \text{ pc}^{-3} \text{ km}^{-3} \text{ s}^3$, if about 1/3 of the gas eventually turns into stars and the rest of the central gas is driven away. Dissipationless merging of the stellar components of such disks would create galaxies with core phase densities comparable to the most massive, lowest Q_0 , early type galaxies (Carlberg 1986). For disks in the same potential, but with lower surface mass densities that phase density will be higher. That is, in a plane parallel sheet $\pi G \Sigma h = \sigma^2$, $Q_d \propto \Sigma^2 \sigma^{-5}$. To keep the Toomre disk stability parameter (Toomre 1964) near unity, requires that the velocity dispersion adjust in proportion to the surface mass density, $\sigma \propto \Sigma$. Therefore $Q_d \propto \sigma^{-3}$. The minimum velocity dispersion of a galactic disk is approximately 10 km s^{-1} , due to stirring of molecular clouds and internal motions of dissolving star clusters, so the highest phase density that merging disks would create would be $\simeq 10^{-3} \text{ M}_\odot \text{ pc}^{-3} \text{ km}^{-3} \text{ s}^3$. Therefore a pure disk merger scenario could account for the core phase densities of all the cored, $\gamma' < 0.3$, early type galaxies but cannot account for the higher phase densities of the early type-galaxies with power-law cores. This is not to dismiss the important role that core scouring likely also plays, as discussed below.

Assuming that all early type galaxies do begin with fairly flat cores, a widely discussed mechanism for subsequent core buildup is that globular clusters can be dragged into the centers of galaxies (Tremaine et al. 1975). Although the current globular cluster population is insufficient to provide the required mass, it is likely that at high redshift significantly more high mass clusters were present, which evolved under the action of various dynamical processes that have been studied and tested extensively (Murali & Weinberg 1997a,b; Fall & Zhang 2001; McLaughlin & Fall 2008; Gieles 2009; Larsen 2009; Chandar et al. 2010; Fall & Chandar 2012). Allowing for the evolution of the globular cluster population can build up all of the nuclear star cluster mass in galaxies with stellar masses below about 10^{11} M_\odot (Antonini et al. 2012; Antonini 2013).

The phase density can be used for a rough calculation of the accreted globular cluster mass. As discussed with Equation 8, the phase density at the maximum radius from which globular clusters can spiral in is $Q \gtrsim 4 \times 10^{-6} \text{ M}_\odot \text{ pc}^{-3} \text{ km}^{-3} \text{ s}^3$, at which phase density the interior stellar mass of $\simeq 2.0 \times 10^{10} \text{ M}_\odot$, which can be read off Figure 5. For the greatly enhanced progenitor globular cluster to stellar mass fraction of 0.04 that Gnedin et al. (2013) suggest, the accreted mass will be $8 \times 10^8 \text{ M}_\odot$ which spirals down the center to build a core of that mass. Referring to Figure 5 we see that this mass is approximately where the transition value of $Q_0 \simeq 0.003$ that separates power-law from cored early type galaxies occurs. The globular cluster population enhancement, which only needs to apply to the inner kiloparsec or so, is about a factor of ten over current epoch galaxies have an average of approximately 0.003 of

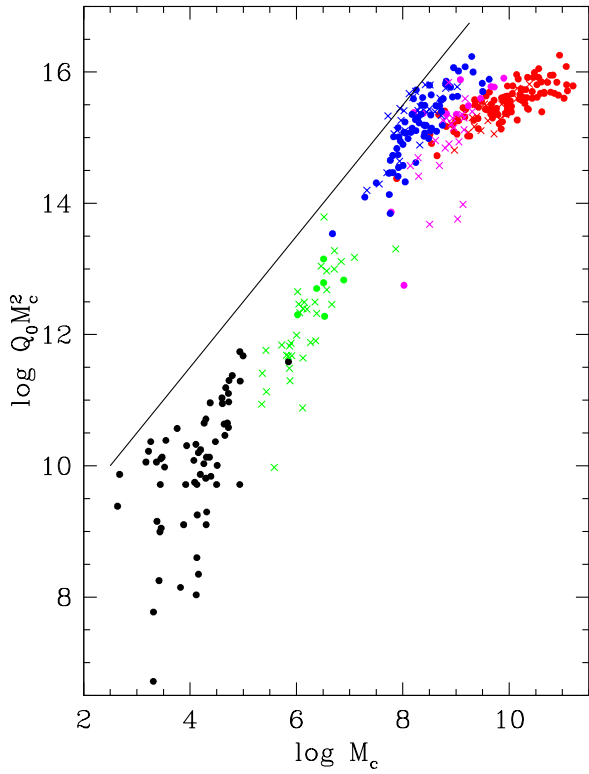


FIG. 9.— The phase space density scaled with the core mass squared, in which mergers move as $Q_0 M_c^2 \propto M_c^{3\beta}$. The symbols are as in Figure 1. A line of constant density, $Q_0 M_c^2 \propto \rho^{1/2} M_c$, is shown.

their stellar mass in globular clusters (Harris et al. 2013). Outside the core the stellar density distribution that is providing the friction generally falls faster than the core mass - core radius relation so smaller cores, which have higher Q_0 , will bring in fewer clusters. Since the available globular cluster mass is proportional to the galaxy mass, the inspiralled globular cluster mass will scale in proportion to the core mass, Figure 6. A second constraint on the progenitor globular cluster population is that it must have significant net rotation to produce the rotation of power law cores, Figure 7.

The detailed calculations of Gnedin et al. (2013) predict that the excess mass in the core relative to the galaxy mass should be proportional to the inverse square galaxy mass, comparable to the excess mass-velocity dispersion relation of Antonini (2013). To test this prediction we calculate ΔM_c as the difference between Equations 4 and a constant density core. We define ΔM_c as $M_c(\gamma') - M_c(\gamma' = 0)$. The correlation between the logarithms of $\Delta M_c/M_*$ and M_* , the stellar mass of the galaxy, is a very weak $r = -0.33$ for all the ATLAS3D galaxies. Restricting the fit to the galaxies with $\gamma' > 0.3$, *i. e.* all non-cored galaxies, the slope of the $\log \Delta M_c/M_* - \log M_*$ relation is -0.52 ± 0.13 , in accord with the predicted inverse square root relation (Gnedin et al. 2013) but the correlation rises to only a marginal -0.49 . Although it seems inevitable that a substantial number of globular clusters have spiralled into galactic

cores, the predicted relation between ΔM_c and M_* accounts for only about 11% of the variance. Of course galaxy to galaxy differences in formation history, central globular cluster numbers, and the specific properties of the globulars from one galaxy to another could account for the scatter.

5.2.2. The Core Scouring Scenario

All early type galaxies could be created with fairly steep power-law cores, which then requires a mechanism to hollow out the cores in larger galaxies. Super-massive black holes pairs that come together after two progenitor galaxies merge will quickly sink into the core (Begelman et al. 1980). Stars that encounter the pair can be ejected from the core to “scour” out of a power law core and produce a much shallower central density profile (Ebisuzaki et al. 1991; Faber et al. 1997; Milosavljević & Merritt 2001). The process preferentially depletes stars on radial orbits to leave a relatively tangential velocity ellipsoid in the core (Quinlan & Hernquist 1997; Milosavljević & Merritt 2001; Antonini et al. 2012). Kinematic observations of a sample of cored early type galaxies do show the expected signature (Thomas et al. 2013). Simulations have shown that a single binary black hole pair ejects only a few times the resulting merged black hole mass, so the small M_{BH}/M_c ratios of cored galaxies require multiple mergers to successfully scour the core (Faber et al. 1997; Milosavljević & Merritt 2001; Merritt 2006; Gualandris & Merritt 2008; Dullo & Graham 2013).

Kormendy & Bender (2013) present observational arguments for a scenario in which subsequent nearly dissipationless major merging dominates the formation of the most massive early type galaxies, as indicated by the very slow rise of central velocity dispersion with increasing mass. Their Faber-Jackson relations for core and power-law galaxies can be translated into the core phase density - core mass relation which we present. The core scouring model at present does not address the strong correlation between the core profile slope γ' and the core phase density. Since power-law core galaxies also contain black holes they too should have been subject to core-scouring, but many of them have sufficiently high core phase densities that a power law core can be maintained or rebuilt (Bahcall & Wolf 1976; Merritt & Szell 2006; Merritt 2009). Core scouring certainly plays some role which can vary from galaxy between creating the core to largely one of maintaining a shallow profile.

6. CONCLUSIONS

The coarse grain core phase density, Q_0 , of early type galaxies provides dynamical insight into the properties of the galactic cores and serves as a dynamical ordering parameter. The core phase density and the slope of the core brightness profile, γ' , are very strongly correlated, $r = 0.83$. We also find that for the standard definitions of cored and power-law profiles, $\gamma' < 0.3$ and $\gamma' > 0.5$, respectively, then Q_0 does a very good job of separating the two distributions, although there is a substantial intermediate core slope population between the two. The transition from power-law and cored elliptical occurs around $Q_0 \simeq 0.003 M_\odot \text{pc}^{-3} \text{km}^{-3} \text{s}^3$. Q_0 correlates significantly but less strongly with the galaxy rotation, the ratio of the central black hole mass to the core mass,

and quite weakly with the fraction of dark matter inside the effective radius.

Primordial cores could have been built as power-laws through dissipative star formation or as relatively low density cored profiles through disk merging. The two main models for subsequent core evolution, globular cluster inspiral and core scouring by black hole binary pairs, are considered relative to the phase space density correlations. We find that the predicted relation between excess mass above a flat core and galaxy stellar mass is present in the power-law and intermediate slope cores but with considerable scatter. In a diagram of Q_0 weighted with the M_c^2 as a function of M_c the power-law cores are the high mass end of a sequence from globular clusters through Nuclear Star Clusters. The sequence has slowly rising core density with mass, roughly as simulations of tidal dissolution of globular clusters have found. The cored early types are on a much shallower relation, about as would be expected from major merg-

ers. The transition Q_0 between power-law and cored early types can be understood as the maximum possible power-law core that can be built from the greatly enhanced globular cluster population at high redshift present in the largest cored early type galaxy. Core scouring clearly plays a role in maintaining fairly flat core profiles, but offers no ready explanation for the fairly abrupt disappearance of cored galaxies at a phase density of $Q_0 = 0.003 M_\odot \text{pc}^{-3} \text{km}^{-3} \text{s}^3$.

We conclude that no single model completely explains the core slope-phase density relationship, although a combination of stellar dynamical effects seems likely to be the mechanism which leaves an indicative signature in the strong correlation with core phase density.

This research was supported by CIFAR and NSERC Canada. We thank an anonymous referee and Davor Krajnović for comments.

REFERENCES

- Antonini, F., Capuzzo-Dolcetta, R., Mastrobuono-Battisti, A., & Merritt, D. 2012, *ApJ*, 750, 111
- Antonini, F. 2013, *ApJ*, 763, 62
- Barnes, J. E. 1988, *ApJ*, 331, 699
- Bahcall, J. N., & Wolf, R. A. 1976, *ApJ*, 209, 214
- Begelman, M. C., Blandford, R. D., & Rees, M. J. 1980, *Nature*, 287, 307
- Binggeli, B., Sandage, A., & Tarengi, M. 1984, *AJ*, 89, 64
- Binney, J., & Merrifield, M. 1998, *Galactic astronomy*, Princeton University Press, Princeton
- Binney, J., & Tremaine, S. 2008, *Galactic Dynamics: Second Edition*, Princeton University Press, Princeton
- Böker, T., Sarzi, M., McLaughlin, D. E., et al. 2004, *AJ*, 127, 105
- Carlberg, R. G. 1986, *ApJ*, 310, 593
- Carollo, C. M., Franx, M., Illingworth, G. D., & Forbes, D. A. 1997, *ApJ*, 481, 710
- Cappellari, M., Emsellem, E., Krajnović, D., et al. 2011, *MNRAS*, 413, 813
- Cappellari, M., Scott, N., Alatalo, K., et al. 2013, *MNRAS*, 432, 1709
- Cappellari, M., McDermid, R. M., Alatalo, K., et al. 2013, *MNRAS*, 432, 1862
- Capuzzo-Dolcetta, R., & Miocchi, P. 2008, *ApJ*, 681, 1136
- Chandar, R., Fall, S. M., & Whitmore, B. C. 2010, *ApJ*, 711, 1263
- Côté, P., Piatek, S., Ferrarese, L., et al. 2006, *ApJS*, 165, 57
- Côté, P., Ferrarese, L., Jordán, A., et al. 2007, *ApJ*, 671, 1456
- Cox, T. J., Dutta, S. N., Di Matteo, T., et al. 2006, *ApJ*, 650, 791
- Crane, P., Stiavelli, M., King, I. R., et al. 1993, *AJ*, 106, 1371
- Djorgovski, S., & Davis, M. 1987, *ApJ*, 313, 59
- Dullo, B. T., & Graham, A. W. 2012, *ApJ*, 755, 163
- Dullo, B. T., & Graham, A. W. 2013, *ApJ*, 768, 36
- Ebisuzaki, T., Makino, J., & Okumura, S. K. 1991, *Nature*, 354, 212
- Emsellem, E., Cappellari, M., Peletier, R. F., et al. 2004, *MNRAS*, 352, 721
- Emsellem, E., Cappellari, M., Krajnović, D., et al. 2007, *MNRAS*, 379, 401
- Emsellem, E., Cappellari, M., Krajnović, D., et al. 2011, *MNRAS*, 414, 888
- Faber, S. M., & Jackson, R. E. 1976, *ApJ*, 204, 668
- Faber, S. M., Tremaine, S., Ajhar, E. A., et al. 1997, *AJ*, 114, 1771
- Fall, S. M., & Zhang, Q. 2001, *ApJ*, 561, 751
- Fall, S. M., & Chandar, R. 2012, *ApJ*, 752, 96
- Ferrarese, L., van den Bosch, F. C., Ford, H. C., Jaffe, W., & O’Connell, R. W. 1994, *AJ*, 108, 1598
- Ferrarese, L., & Merritt, D. 2000, *ApJ*, 539, L9
- Ferrarese, L., Côté, P., Jordán, A., et al. 2006, *ApJS*, 164, 334
- Gebhardt, K., Richstone, D., Ajhar, E. A., et al. 1996, *AJ*, 112, 105
- Gebhardt, K., Bender, R., Bower, G., et al. 2000, *ApJ*, 539, L13
- Genzel, R., Newman, S., Jones, T., et al. 2011, *ApJ*, 733, 101
- Genzel, R., Förster Schreiber, N. M., Lang, P., et al. 2014, *ApJ*, 785, 75
- Glass, L., Ferrarese, L., Côté, P., et al. 2011, *ApJ*, 726, 31
- Gieles, M. 2009, *MNRAS*, 394, 2113
- Gnedin, O. Y., Ostriker, J. P., & Tremaine, S. 2013, *arXiv:1308.0021*
- Goldstein, H., Poole, C., & Safko, J. 2002, *Classical mechanics* (3rd ed.) Addison-Wesley, San Francisco
- Graham, A. W., & Guzmán, R. 2003, *AJ*, 125, 2936
- Graham, A. W., Erwin, P., Trujillo, I., & Asensio Ramos, A. 2003, *AJ*, 125, 2951
- Graham, A. W., & Scott, N. 2013, *ApJ*, 764, 151
- Gualandris, A., & Merritt, D. 2008, *ApJ*, 678, 780
- Harris, W. E. 1996, *AJ*, 112, 1487
- Harris, W. E., Harris, G. L. H., & Alessi, M. 2013, *ApJ*, 772, 82
- Hartmann, M., Debattista, V. P., Seth, A., Cappellari, M., & Quinn, T. R. 2011, *MNRAS*, 418, 2697
- Hilz, M., Naab, T., Ostriker, J. P., et al. 2012, *MNRAS*, 425, 3119
- King, I. R. 1966, *AJ*, 71, 64
- King, I. 1962, *AJ*, 67, 471
- King, I. R. 1978, *ApJ*, 222, 1
- Kormendy, J. 1985, *ApJ*, 292, L9
- Krajnović, D., Emsellem, E., Cappellari, M., et al. 2011, *MNRAS*, 414, 2923
- Kormendy, J., Dressler, A., Byun, Y. I., et al. 1994, *European Southern Observatory Conference and Workshop Proceedings*, 49, 147
- Kormendy, J., & Bender, R. 2013, *ApJ*, 769, L5
- Krajnović, D., Karick, A. M., Davies, R. L., et al. 2013, *MNRAS*, 433, 2812
- Larsen, S. S. 2009, *A&A*, 494, 539
- Lauer, T. R. 1985, *ApJ*, 292, 104
- Lauer, T. R., Ajhar, E. A., Byun, Y.-I., et al. 1995, *AJ*, 110, 2622
- Lauer, T. R., Gebhardt, K., Faber, S. M., et al. 2007, *ApJ*, 664, 226
- Lauer, T. R., Faber, S. M., Richstone, D., et al. 2007, *ApJ*, 662, 808
- Lauer, T. R. 2012, *ApJ*, 759, 64
- Loose, H. H., Kruegel, E., & Tutukov, A. 1982, *A&A*, 105, 342
- Magorrian, J., Tremaine, S., Richstone, D., et al. 1998, *AJ*, 115, 2285
- McConnell, N. J., & Ma, C.-P. 2013, *ApJ*, 764, 184
- McLaughlin, D. E., King, A. R., & Nayakshin, S. 2006, *ApJ*, 650, L37
- McLaughlin, D. E., & Fall, S. M. 2008, *ApJ*, 679, 1272
- Merritt, D. 2006, *ApJ*, 648, 976
- Merritt, D., & Szell, A. 2006, *ApJ*, 648, 890
- Merritt, D. 2009, *ApJ*, 694, 959
- Merritt, D. 2013, *Dynamics and Evolution of Galactic Nuclei*, Princeton University Press, Princeton
- Milosavljević, M., & Merritt, D. 2001, *ApJ*, 563, 34
- Murali, C., & Weinberg, M. D. 1997, *MNRAS*, 288, 749
- Murali, C., & Weinberg, M. D. 1997, *MNRAS*, 291, 717
- Naab, T., Johansson, P. H., & Ostriker, J. P. 2009, *ApJ*, 699, L178
- Quinlan, G. D., & Hernquist, L. 1997, *New Astronomy*, 2, 533
- Ravindranath, S., Ho, L. C., Peng, C. Y., Filippenko, A. V., & Sargent, W. L. W. 2001, *AJ*, 122, 653
- Rest, A., van den Bosch, F. C., Jaffe, W., et al. 2001, *AJ*, 121, 2431
- Thomas, J., Saglia, R. P., Bender, R., Erwin, P., & Fabricius, M. 2013, *arXiv:1311.3783*
- Toomre, A., & Toomre, J. 1972, *ApJ*, 178, 623
- Toomre, A. 1964, *ApJ*, 139, 1217

- Tremaine, S. D., Ostriker, J. P., & Spitzer, L., Jr. 1975, ApJ, 196, 407
- Trujillo, I., Erwin, P., Asensio Ramos, A., & Graham, A. W. 2004, AJ, 127, 1917
- Turner, M. L., Côté, P., Ferrarese, L., et al. 2012, ApJS, 203, 5
- Walcher, C. J., van der Marel, R. P., McLaughlin, D., et al. 2005, ApJ, 618, 237